Annals of Nuclear Energy 76 (2015) 27–39

Contents lists available at ScienceDirect

Annals of Nuclear Energy

journal homepage: www.elsevier.com/locate/anucene

Coupling of dynamic Monte Carlo with thermal-hydraulic feedback

Bart L. Sjenitzer [a,c,*], J. Eduard Hoogenboom [a], Javier Jiménez Escalante [b], Victor Sanchez Espinoza [b]

[a] Delft University of Technology, Mekelweg 15, 2629JB Delft, The Netherlands
[b] Karlsruhe Institute of Technology (KIT), Hermann-von-Helmholtz-Platz 1, 76344 Eggenstein-Leopoldshafen, Germany
[c] SCK•CEN, Belgian Nuclear Research Centre, Boeretang 200, BE-2400 Mol, Belgium

ARTICLE INFO

Article history:
Received 2 April 2014
Received in revised form 8 September 2014
Accepted 9 September 2014
Available online 6 October 2014

Keywords:
Monte Carlo
Neutron transport
Coupled calculation
Feedback
Thermal-hydraulics

ABSTRACT

Transient analysis of nuclear reactors is traditionally the domain of deterministic methods, even tough these methods are known to have limitations. With the development of dynamic Monte Carlo and the development of coupled-steady state Monte Carlo calculations the road has been paved to perform transient analysis of high power reactors using Monte Carlo. By this way, it is possible to take into account the thermal-hydraulic feedback, while the neutron transport is modelled in full detail.

In this paper a new method is described, which can perform such stochastic analysis of a transient scenario.

1. Introduction

One of the most important aspects for transient analysis is the thermal-hydraulic feedback. This feedback mechanism is essential for the safe operation of nuclear reactors. For example, when the temperature in a light water reactor increases, the density of the moderator decreases and neutrons will be less moderated, causing, in general, a reactivity decrease. When the reactivity becomes negative, the power produced will be reduced, which lowers the temperature of the reactor. There are many of these feedback mechanisms, some positive and some negative and for the design of a nuclear reactor, it is crucial to take these effects into account. These effects determine the time dependent behaviour of a reactor and therefore the maximum temperatures reached during a transient.

To incorporate these feedback mechanisms into a neutronics calculation, it is common to couple a thermal-hydraulics code to a neutronics code. A thermal-hydraulics code calculates the density profile of the coolant and the temperature profile in the reactor using heat-transfer models and the new material properties are then used for the neutronics calculation. An elaborate description of the methods currently applied can be found in D'Auria et al. (2004).

1.1. Deterministic coupled transient calculations

With the ever increasing computing power, many new developments can be found, which couple a deterministic neutronics solver to a thermal-hydraulics solver. The neutronics solver can be, for example, a nodal code (Vedovi et al., 2004), or, more advanced, use the method of characteristics (Hursin et al., 2011) and these codes can be either internally or externally coupled to the thermal-hydraulics code. The advantage of external coupling is the limited adjustments needed to the codes; they can stay autonomous. With internal coupling on the other hand, the two codes are merged into one code, which is usually faster and therefore possibly more accurate, but this requires more adjustments and the merged code must be validated separately. The external coupling is becoming a standard calculation technique for the analysis of transients in a light water reactor (Peltonen and Kozlowski, 2011), but it is also done for less common reactor types such as the high temperature reactor (Boer et al., 2010) or the molten salt reactor (Kópházi et al., 2009).

A downside of coupling a deterministic neutronics solver with a thermal-hydraulics solver, is the limited accuracy of the deterministic method. When a deterministic neutronics calculation is done, there is always a number of approximations applied, such as discretisation in time, space, energy and angle. Also, more fundamental approximations might be needed, such as homogenisation or application of diffusion theory, which makes it difficult to estimate the error in such calculations. It is possible to verify the final result with a stand-alone Monte Carlo calculation (Broeders et al.,

* Corresponding author at: SCK•CEN, Belgian Nuclear Research Centre, Boeretang 200, BE-2400 Mol, Belgium.
E-mail address: Bart.Sjenitzer@SCKCEN.be (B.L. Sjenitzer).

http://dx.doi.org/10.1016/j.anucene.2014.09.018
0306-4549/

2003), but this is only possible if the temperatures and densities are known.

1.2. Coupled Monte Carlo thermal-hydraulics calculations

A recent development in the field of coupled calculations is the coupling between a Monte Carlo neutronic calculation and thermal-hydraulic analysis. Presently this can be achieved only for steady-state calculations, with a fixed power level. Therefore, only the thermal-hydraulic effects that influence the power profile in a reactor are taken into account in the Monte Carlo calculation and the feedback mechanisms that influence the total power are neglected; only the static effect on the reactivity can be analysed, neglecting the dynamic nature of the feedback.

The first occurrence in the literature of the coupling of a Monte Carlo neutronics code with a thermal-hydraulics code was in 2003, when MCNP4C was coupled with SIMMER-III by Mori et al. (2003), but in this case there is no iterative process. The thermal-hydraulics code SIMMER is run once to calculate the temperature profile for MCNP.

Next, in 2004 Bakanov et al. (2004) coupled TDMCC with STAR-CD, but there is little description of the method. A demonstration has been given of a coupled calculation of a fuel assembly, but there is no discussion on the accuracy of the calculation. Joo et al. (2004) used MCCARD to verify the DeCART transport code, both coupled with a simplified feedback script. Here the results of a coupled analysis of a mini core seem to match relatively well between MCCARD and DeCART.

Next, coupling methods have become part of research tools, with the coupling of stand-alone codes, such as MCNP and STAFAS. Waata et al. (2005a) implemented this method to analyse the HPLWR (Waata et al., 2005b).

Meanwhile, the developments continued, focusing on an increased efficiency of the neutronics calculation, with Tippayakul et al. (2008) who used a nodal code to improve fission source convergence, Sanchez and Al-Hamry (2009) worked on the improvement of the convergence of the coupled solution and the mapping between the two codes is further optimised by Seker et al. (2007a). A different direction of research is to develop partly internal coupling (Leppänen et al., 2012) or complete internal coupling investigated by Griesheimer et al. (2008). In these works (some) thermal-hydraulics models are integrated in the Monte Carlo code.

The most recent developments focus on increasing the flexibility of the coupling scheme, making it generally applicable (Hoogenboom et al., 2011; Ivanov et al., 2011) and extension of the coupled calculations to whole-core applications (Kotlyar et al., 2011; Vazquez et al., 2012). The hybrid deterministic/stochastic method which increases the efficiency of the Monte Carlo calculation is further developed by Espel et al. (2013).

1.3. Coupled Dynamic Monte Carlo

This work combines the coupled calculations with the transient calculations in order to perform transient calculations including feedback, using only a Monte Carlo approach for the neutronics part of the calculation.

The Monte Carlo code is coupled to a sub-channel code, which is a fast thermal-hydraulics code, but not a high-fidelity code. Although it might seem more logical to couple a computational-expensive high-fidelity neutronics code to a high-fidelity thermal-hydraulics code, the efficiency of the sub-channel code is more useful during the development of a new method. The theory can be extended easily to any kind of external code, including a high-fidelity computational fluid dynamics (CFD) code (Seker et al., 2007b).

First the theory of the coupling is discussed, next there are three test cases: a proof of principle in simplified geometry, a pin cell on a long time scale and a mini core in a short time scale with a strong transient.

2. Theory

To couple Monte Carlo to thermal-hydraulics in a transient calculation first the initial conditions must be calculated and from this starting point the coupled transient part is started. The possible schemes to do this are discussed in Section 2.1.

The other challenges are specific for Monte Carlo: variance estimation and temperature dependent cross sections. When performing a coupled calculation it should be acknowledged that part of the calculation is not stochastic and this can influence the variance estimation. The implications are discussed in Section 2.3. As the coupling will also create a large number of temperatures, different methods to handle this broad range are discussed in Section 2.4.

2.1. Coupling scheme

In nuclear reactor modelling, it is common to use an operator-splitting technique to solve a multi-physics problem. Although this approach does not take into account the non-linearities which are present in a typical coupled reactor physics problem (Ragusa and Mahadevan, 2009), it is a logical place to start the development of a new coupling technique. When the possibility of coupling Monte Carlo with thermal-hydraulic feedback is demonstrated, more advanced coupling schemes can be investigated.

There are three ways of coupling the thermal-hydraulics calculation and the neutronics calculation: implicit, semi-implicit and explicit. The implicit scheme iterates the coupled codes per time interval until the combined codes have converged. When converged the scheme will continue to the next time interval, as depicted in Fig. 1. The advantage of this scheme is that it can be unconditionally stable, which allows for larger time intervals. However, the downside of this scheme is that it requires major alterations to the existing solvers to allow for the iteration steps. Also, there is a lot of data exchange between the coupled codes and therefore this scheme is usually implemented using internal coupling, making the implementation even more complex. A first attempt was made by Mahadevan et al. (2011) to use a Jacobian-free Newton–Krylov method to perform implicitly coupled calculations with the code system KARMA. On the other hand Watson and Ivanov (2012) incorporated implicit coupling in the TRACE/PARCS code system by explicitly forming the full Jacobian matrix and solving for a global residual.

For the semi-implicit method, the calculation of the current time interval is partly based on data of the previous time interval and partly on the data of the current time interval. For example, when the TRAC-PF1/NEM code calculates the fluxes and the power production, it uses coolant temperatures and densities of the current time interval, but fuel rod temperatures of the previous time interval (Ivanov and Avramova, 2007).

In most cases the explicit coupling scheme is used, since this is the easiest to implement and codes do not have to be altered, so validated codes can be used. Also, it is a fast method since there is no iteration involved, allowing the use smaller time intervals. When using this method one should beware that the time interval is small enough to ensure stability.

The temperature and density profiles are calculated with the thermal-hydraulics code and with these profiles the power distribution is calculated. This power distribution is then used in the thermal-hydraulics code. This scheme is depicted is Fig. 2 and this is also the scheme used in this work, because of its calculation speed and the possibility to couple externally.

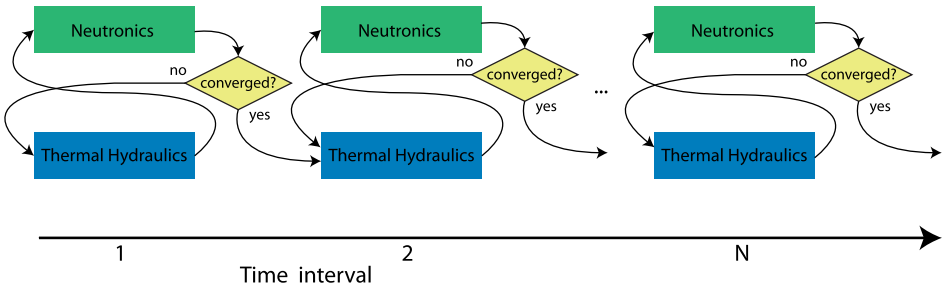

Fig. 1. Scheme for an implicit coupling of the neutronics solver and the thermal-hydraulics solver. In this case, each time interval has to converge before continuing to the next interval.

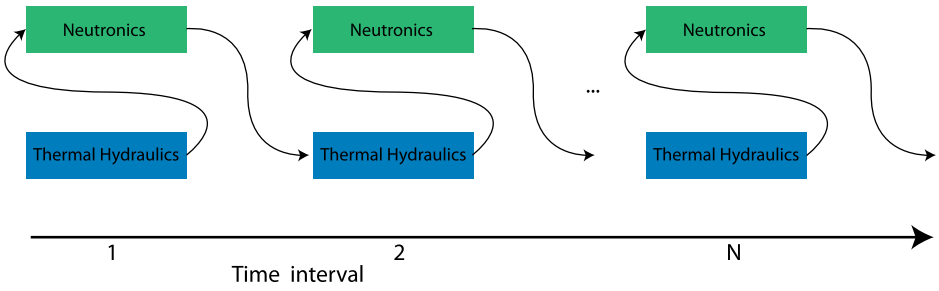

Fig. 2. Scheme for an explicit coupling of the neutronics solver and the thermal-hydraulics solver. In this case, first the thermal-hydraulic conditions are calculated and then the power distribution.

2.1.1. Coupling coefficients

In a normal coupled calculation using two deterministic codes, the explicit coupling scheme can be depicted as follows:

$$T^{n+1} = T^n + \Delta t \frac{\mathrm{d}T}{\mathrm{d}t}(P^n) \tag{1}$$

$$P^{n+1} = P^n + \Delta t \frac{\mathrm{d}P}{\mathrm{d}t}(T^{n+1}) \tag{2}$$

Here P is the power profile resulting from the neutronics calculation and T is the temperature and density profile resulting from the thermal-hydraulics calculation. The superscript n indicates that the values are to be taken at the start of time interval n.

When doing a Monte Carlo calculation, it is important to realise that the code will not calculate the power in a single point in time. In fact, the output of a Monte Carlo calculation is the total energy E released during the time interval:

$$E^{n+\frac{1}{2}} = \int_t^{t+\Delta t} P(T^n, t)\mathrm{d}t \tag{3}$$

From the total energy released during the time interval, an average power can be calculated over the time interval. This average can then be extrapolated to a power level at the boundary of the next time interval. When assuming a linear increase this becomes:

$$P^{n+1} = \frac{2E^{n+\frac{1}{2}}}{\Delta t} - P^n \tag{4}$$

This power distribution can be used for the thermal-hydraulics calculation.

2.2. Practical implementation of the coupling scheme

A transient calculation consists of two parts: the calculation of the initial conditions and the actual transient. To calculate the initial conditions, a coupled steady-state calculation is used, which is based on the method developed by Hoogenboom et al. (2011). This method has been extended to calculate the critical conditions, which is in the case of a pressurised water reactor the critical boron concentration, but for other types of reactors this could be adjusted to calculate for example the critical control-rod position. Also the fission source convergence has been improved.

When using this method, the steady-state total-power level is set externally and then the temperature and density profiles are calculated with the thermal-hydraulics code. With these profiles, a Monte Carlo calculation is started, calculating a new power profile and k_{eff}. After this calculation, three modification are made to the input of the Monte Carlo calculation. First, the new temperature and density profiles are calculated using the thermal-hydraulics code and the Monte Carlo input is updated with these new temperatures and densities.

Secondly, the new boron concentration, C_{boron}, is calculated by a linear extrapolation of the concentration from the two previous iterations. As explained before, for pressurised water reactors a critical boron concentration is calculated, but the method can also be used to calculate a different critical condition, e.g. a critical control-rod position. For iteration number m this is calculated using:

$$C_{m,\mathrm{boron}} = C_{m-1,\mathrm{boron}} - \frac{k_{\mathrm{eff}\,m-1} - 1}{k_{\mathrm{eff}\,m-1} - k_{\mathrm{eff}\,m-2}}\left(C_{m-1,\mathrm{boron}} - C_{m-2,\mathrm{boron}}\right) \tag{5}$$

For the first two cycles an initial guess is needed.

Thirdly, the accuracy is increased if the following condition is met:

$$|k_{\mathrm{eff}} - 1| < 2\sigma_{k_{\mathrm{eff}}} \tag{6}$$

with $\sigma_{k_{\mathrm{eff}}}$ the standard deviation of k_{eff}. In this case the number of active batches is increased by a factor of two. This allows for the first iteration steps to use less calculation time and only increase accuracy when needed. There are more advanced schemes under development to optimise this iteration process (Dufek and Gudowski, 2006), improving not only the way the accuracy is increased, but also the way the temperatures and densities are sampled. This new method might be extended to improve the estimation of the correct boron concentration. However, for this demonstration, a simple scheme suffices.

Also, the fission sources of the last cycle are stored to use for the next iteration, which reduces the number of inactive cycles needed to reach a converged source. Since the difference in fission source profile between two iterations is not very large, the final fission source of the previous iteration is a good initial guess for the present iteration.

In the second part of the calculation, the actual transient is simulated, using the temperature and density profiles calculated in the first part as initial conditions. This method is based on the methodology described by Sjenitzer and Hoogenboom (2013). First, a dynamic neutron and precursor source is sampled using a classical steady-state calculation. Then, the first time interval is calculated using the dynamic Monte Carlo method. The calculated power profile is then transferred to the thermal-hydraulics code, which calculates the temperature and density profiles for the new time interval. These are returned to the Monte Carlo code to continue with the next time interval. The Monte Carlo calculation is split in batches of neutrons and for each batch a separate thermal-hydraulics calculation is performed. First all time intervals of a batch are completed, before continuing to the next batch.

2.3. Variance estimation

The mean result in a Monte Carlo calculation is a stochastic variable, which has a normal distribution according to the central limit theorem and usually the variance is estimated between (groups of) neutron histories. However, in a coupled calculation neutrons are no longer uncorrelated, due to the thermal-hydraulic feedback, making the central limit theorem no longer applicable.

This can be overcome by performing the thermal-hydraulics calculation for each batch of neutrons separately. In this case, the variance can be estimated between the different, statistically independent, batches. This way, also the propagation of the variance between time intervals is taken into account and the statistical uncertainty introduced by the coupling will be included. However, it does not take into account any bias, either in the thermal-hydraulics code or in the geometrical description. Another downside is that the feedback is calculated on smaller sample sizes, which might prove unreliable.

Also, if the thermal-hydraulic feedback has a strong non-linear behaviour, such as a step-like response function, this cannot be taken into account. Only the average response of all possible outcomes is tallied. An example where such effects are prominent is the simulation of instabilities in a supercritical-water reactor (T'Joen and Rohde, 2012). Here this coupling strategy could yield a non-physical result: an average of the power oscillations. In such a case, it could be more useful to estimate the maximum power per batch or to study the distribution of batch results.

For coupled burnup calculations Dumonteil and Diop (2011) have demonstrated that the result of a coupled calculation might be biased when the estimator is not properly corrected for the non-linearity of the coupled equations. For the Bateman equations it is possible to find an analytical solution for the correction factor, but when coupling Monte Carlo to a thermal-hydraulics code, this will prove difficult. This is not only a problem for transient analysis, but also when doing steady-state calculations. Since the calculations in this paper do not include regimes with two-phase flow, it is assumed that the mean and variance are unbiased.

2.4. Generation of temperature dependent cross sections

One of the major challenges for a coupled Monte Carlo calculation is the temperature dependence of cross sections (Brown et al., 2008). Although it is theoretical possible to generate cross sections at any temperature, it is not feasible to do this for a full-core coupled calculation. In such a calculation there are many nuclides and each nuclide is present at a large range of temperatures; each zone has a different temperature. Therefore, it is common to evaluate the cross sections at 50 K intervals and use for each nuclide two cross-section sets at these preselected temperatures, mixing two versions of the same nuclide to get the correct temperature (Espel et al., 2013; Hoogenboom et al., 2011). This is called stochastic mixing, but it is also known as stochastic interpolation, pseudo materials or temperature interpolation. It is used for all temperature ranges, also in the thermal range where the $S(\alpha,\beta)$ data is of importance.

Currently there are more advanced methods being developed, such as on-the-fly-Doppler broadening which is implemented in MCNP (Yesilyurt et al., 2012) and MONK (Armishaw et al., 2011). Another method to include temperature effects is the explicit treatment of thermal motion, which is being developed for Serpent (Viitanen and Leppänen, 2012) and Tripoli (Zoia et al., 2013). Also direct interpolation of the cross sections is possible, yielding promising results (Sjenitzer, 2009). Although these methods are potentially more accurate, they are still experimental and not widely available. Also, they take more calculation time than the mixing method. Therefore, stochastic mixing is used in this work.

Since the cross-section dependence on temperature is predominant with $\sqrt{T}$ the first mixing schemes used a $\sqrt{T}$ interpolation (Der Marck et al., 2005). Later, Donnelly (2011) showed that the linear interpolation scheme yields similar results, if not slightly more accurate. Therefore the linear-interpolation scheme will be used in the current work.

3. Practical implementation and demonstration

The demonstration of the coupling between the Monte Carlo neutronics calculation and the thermal-hydraulics calculation is done in three steps. First, a simplified model is created to study the feasibility of coupling Monte Carlo with feedback mechanisms and to investigate the impact of the variance on the stability of the calculation.

Next, a more realistic case is simulated, coupling the power profile in a single fuel pin with a realistic thermal-hydraulics model. This calculation is performed on a seconds to minutes time scale, investigating the feasibility of doing a realistic coupled calculation and studying the effect of variance on the thermal-hydraulics code. Finally, an analysis on a mini-core benchmark has been performed to demonstrate the method in a realistic geometry and to verify the results obtained.

3.1. Second-order feedback model

3.1.1. Problem setup

Lets start with a simplified problem with mono-energetic neutrons, a homogeneous medium and a rectangular 3D geometry. First, a transient is simulated and the results are compared with a point-kinetics calculation. Then, the influence of the stochastics on the feedback is tested. The feedback is incorporated in the total absorption cross section, which is a function of the total power to mimic Doppler broadening, as suggested by Legrady and Hoogenboom (2008):

$$\Delta\Sigma_a = \frac{(P_0 - P_{50\mathrm{ms}})^2}{4P_0^2}\Delta\Sigma_{a,var} \tag{7}$$

Here P_0 is a reference power level, from which the power deviation is calculated and $\Delta\Sigma_{a,var}$ is a scaling variable, which determines the strength of the feedback. P_{50ms} is the average power produced in the last 50 ms. The average over the last 50 ms mimics the time required for the deposited energy to disperse via thermal conduction.

To initiate the transient the total absorption cross section is reduced from 0.5882 to 0.5840 cm^{-1} at $t = 0.2$ s. $\Delta\Sigma_{a,var}$ is set to 0.0042 cm^{-1}, which is equal to the reactivity insertion of 1 \$ and the time interval size is set to 1 ms.

To validate these results the calculation has also been performed with a point-kinetics calculation, with the following feedback incorporated, assuming a linear relation between the reactivity and the total absorption cross section:

$$\Delta\rho = \frac{(P_0 - P_{50\text{ms}})^2}{4P_0^2}\Delta\rho_{var} \tag{8}$$

with $\Delta\rho_{var} = -1\$$.

3.1.2. Results

The power level in the system starts to oscillate after the reactivity insertion as can be seen in Fig. 3. The reactivity insertion is clearly visible and after a short time the negative feedback effect creates a negative reactivity, which reduces the power level, until it has dropped to a level where the reactivity becomes positive again. The results of the point-kinetics calculation agree nicely with the Monte Carlo calculation, also for the long term behaviour as shown in Fig. 4. The oscillations are damped and the power level converges to a new steady state level at $P_{stst} = 3.0P_0$, as expected.

There is a small discrepancy in oscillation period between the Monte Carlo calculation and the point-kinetics calculation, which can use a smaller time interval, updating the feedback coefficient more frequently. This discrepancy is due to the explicit coupling scheme, which always yields a small error proportional to the time interval size. This is not a Monte Carlo specific problem, but an issue for all coupled transient calculations.

Also, the importance of an accurate power tally is investigated. The variance in the power creates a variance in the feedback, which influences the power. To investigate the necessity of an accurate power tally, the feedback is calculated per batch and the number of neutron histories per batch is varied, while the total number of particles is kept constant. This should only influence the accuracy of the feedback, but not the accuracy of the final result. The following batch sizes have been used: 10^4 batches of 10^3 particles, 10^3 batches of 10^4 particles, 10^2 batches of 10^5 particles and a reference solution with a single batch using all 10^7 particles.

It can be seen from Fig. 5 that most batch sizes yield the correct result. However, in the case with only 10^3 particles per batch, the results become biased. It should be noted though, that in this case the average standard deviation in the power tally is 20 %, which is very high. For the case with 10^4 particles per batch the uncertainty drops to 6 %, for 10^5 starting particles the standard deviation is 2 % and in the reference case with all 10^7 neutrons in one batch the standard deviation is 0.2 %. The total variance for the total calculation is the same for all simulations.

This demonstrates that even with relatively high variance, the results are still correct, but caution must be taken. In this example, a statistical uncertainty smaller than 20 % is needed to ensure an unbiased power tally. Although this is only a simple test, with a second-order feedback mechanism, the example does give an indication that such a coupled scheme is valid and robust, when the feedback does not have any discontinuities.

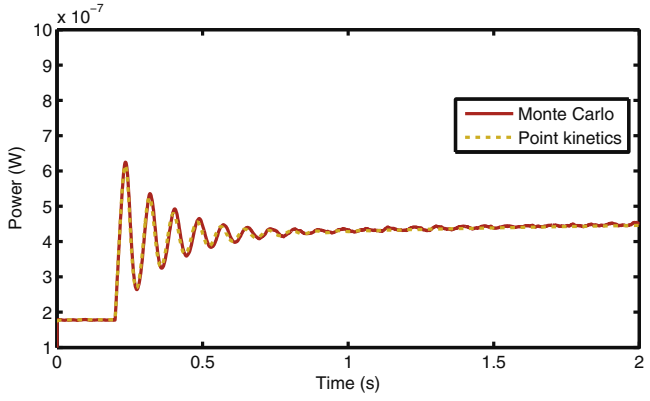

Fig. 3. The power production in a simple system with feedback on a short time scale. After 0.2 s a reactivity insertion is introduced. The oscillating behaviour on a short time scale is correctly predicted by the Monte Carlo method and the point-kinetics method.

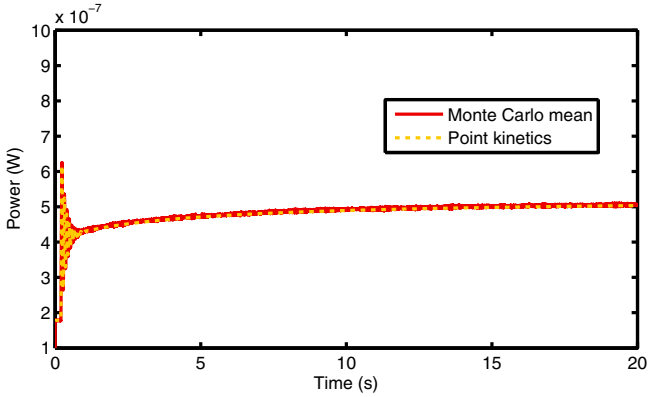

Fig. 4. The power production in a simple system with feedback on a large time scale. After 0.2 s a reactivity insertion is introduced. On a large time scale the Monte Carlo method and the point-kinetics method converge to the same power level.

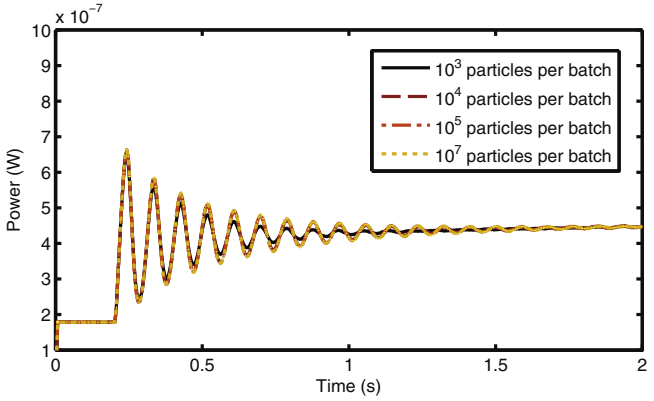

Fig. 5. The power production in a simple system with the feedback coefficients calculated per batch of neutrons. The results are mostly independent of the batch size. However, when the uncertainty in the power is larger than 20%, as in the case with 10^3 particles per batch, the results become biased.

3.2. Pin cell calculation

3.2.1. Problem setup

For the next step in development of a coupled code system, a dynamic version of the general purpose Monte Carlo code Tripoli (TRIPOLI-4 Project Team, 2010) is used, developed by Sjenitzer and Hoogenboom (2013) and this code is coupled with the thermal-hydraulics code SubChanFlow (Imke and Sanchez, 2012). In this example, a coupled calculation is performed on a single fuel pin, which is surrounded by water. The enrichment of the fuel varies axially with higher enriched fuel at the top. The boundary conditions in the x–y plane are periodic and there is a vacuum boundary in the z-direction. The pin cell has been divided into 20 axial regions to capture the axial power profile. The effective

temperature of the fuel rod can be approximated from the surface temperature of the rod, T_s and the centre temperature, T_c (Rowlands, 1962):

$$T_{\text{eff}} = \frac{5}{9}T_s + \frac{4}{9}T_c \tag{9}$$

The layout and dimension are given in Fig. 6, where also the mapping from one code to the other is depicted. In the thermal-hydraulics part the gap between the fuel and the cladding is modelled, but for the Monte Carlo part this gap is neglected as it has virtually no influence on the neutronics. The fuel is made of UO_2, but the enrichment is varied in the axial direction, as plotted in Fig. 7. In this case the system is made critical by adjusting the boron concentration in the coolant, which will yield a relative high boron concentration, since there is no leakage in the x-y plane and no other neutron absorbers.

First, a steady-state situation is calculated using the method described in Section 2.2, yielding the correct initial temperature and density profiles, with a critical boron concentration. Next two transients are simulated. The first transient is a so called zero-transient, where a time-dependent calculation is performed on a critical system, without changing the initial conditions. The second transient which is investigated is initiated by a pump trip, which does create fluctuations in the power level.

3.2.2. Results

After calculating the initial conditions, the zero transient is calculated. The result is shown in Fig. 8, where the coupled calculation is compared with a stand-alone calculation. It can be seen that the initial conditions are not precisely steady state, since the power in the stand-alone calculation starts to decrease slowly

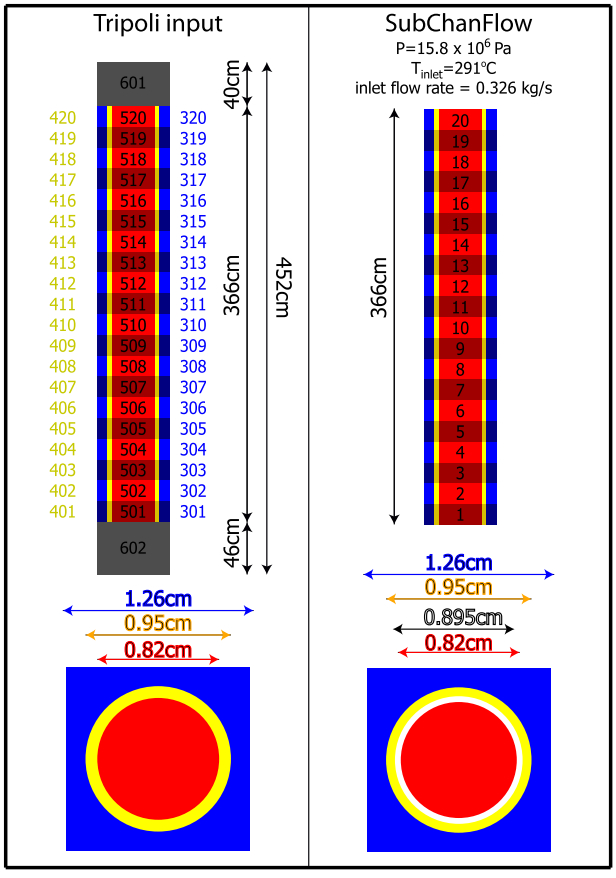

Fig. 6. The neutronic and thermal-hydraulic description of the fuel pin.

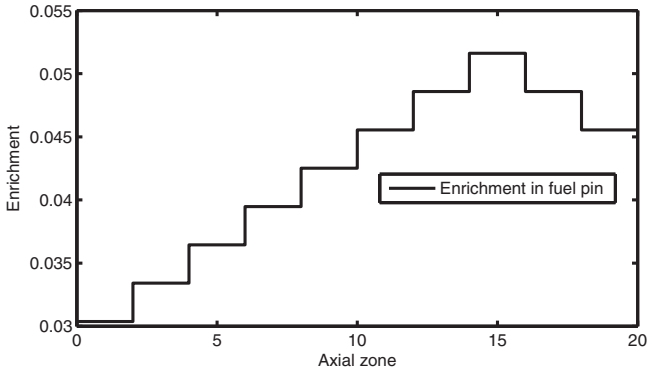

Fig. 7. The system for the numerical example is a small homogeneous cuboid, with mono-energetic neutrons and isotropic scattering. The cuboid is placed in vacuum.

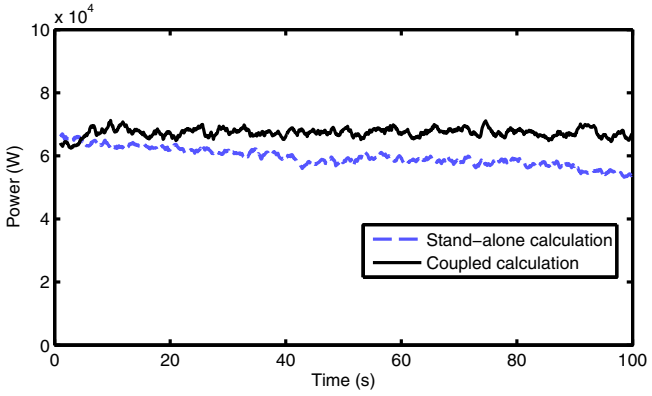

Fig. 8. A zero-transient calculation on an infinite array of fuel pins. The stand-alone calculation slowly decreases in power, but the feedback mechanisms in the coupled calculation keep the power at steady state.

over time. In the coupled case, however, the feedback mechanisms keep the system at a steady state. The differences at the start of the calculations are within the uncertainty observed in the calculation. This simulation demonstrates the stability of a realistic coupled calculation.

Next a pump trip is initiated at $t = 10$ s, which is modelled by a decrease in coolant flow. This initiates an increase in power production, with a peak at $t = 12.5$ s (Fig. 9). After the peak the power stabilises at a new power level. At $t = 40$ s the pump returns to its initial state, with the power level also returning to its original level after some oscillation. The increase in power is to be expected in this specific setup, since the water contains a high amount of boron. When the flow is reduced, the temperature rises and the density of the coolant decreases, which reduces the neutron capture by the boron.

The axial power profile is tallied in 20 zones and the power profiles at different stages during the transient are shown in Fig. 10. Here it can be seen that the main contribution to the total power increase is given by the highly enriched regions, as expected. The flux profile at the start and end of the transient are nearly identical.

It can be seen from Fig. 11 that the transient is indeed driven by the pumping power. Due to the reduced coolant flow, the coolant heats up first, thereby reducing the coolant density leading to an increase of the fuel temperature. During the phases with constant coolant flow, oscillations can be observed where neither the coolant nor the fuel temperature seems to be leading. When the pump flow is returned to nominal, again the coolant properties change first.

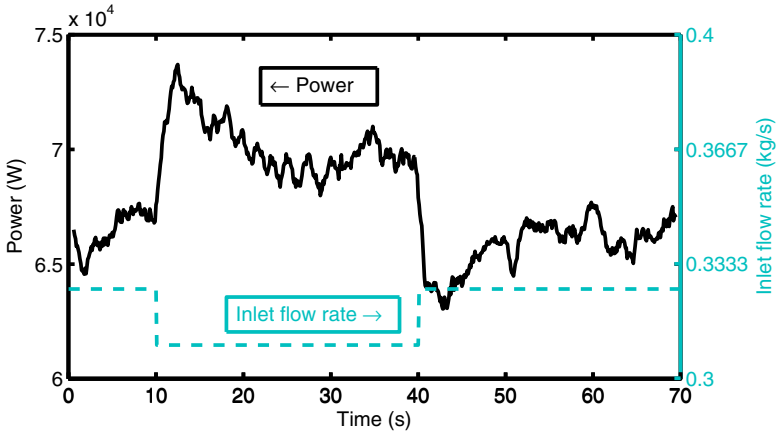

Fig. 9. The evolution of the total power in the fuel pin with a pump trip from 10 s until 40 s. The power excursion due to the reduced pump flow can be observed clearly.

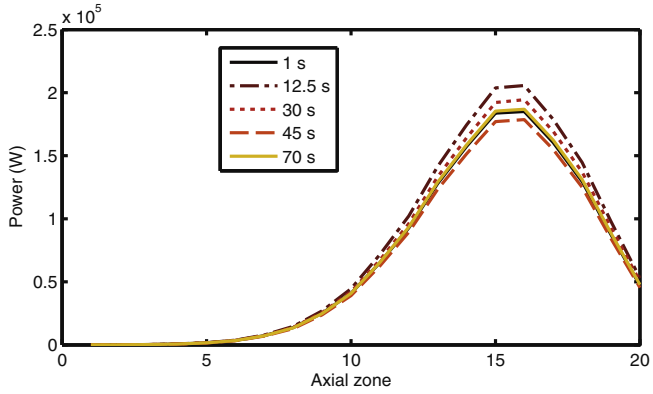

Fig. 10. The axial power profile in the fuel pin at different times during the transient. At 1 s the system is still at steady state, at 12.5 s is the power peak, at 30 s is the new steady state, at 45 s is just after the negative reactivity insertion and at 70 s is the final state, which is similar to the initial state.

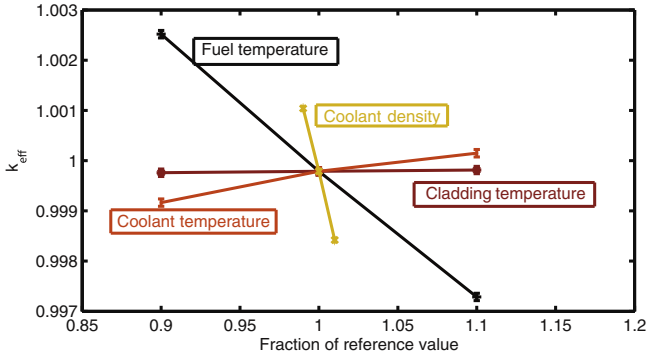

Fig. 12. Feedback coefficients for a pin cell calculated using steady-state calculations.

The size of the power jump can be justified when the feedback coefficients are investigated. In Fig. 12 the feedback coefficients of the material properties are given and it can be seen that after the reduction of pump flow they cancel each other. First, the reduced density and increased temperature of the coolant increase the reactivity and then the Doppler effect in the fuel temperature compensate this increased reactivity.

When the feedback coefficients are calculated from Fig. 12 using linear regression, reactivity contributions of the different material properties can be visualised, Fig. 13. Although this is only an approximate calculation, using average temperatures, it can be seen how the increase in fuel temperature compensates for the reduced coolant density.

Although the results are still somewhat noisy, these examples do demonstrate the feasibility of performing a coupled calculation with Monte Carlo neutronics calculation and a thermal-hydraulics calculation. It is possible to do a calculation on a seconds scale and the effects of the feedback mechanisms can be clearly observed. The noise could possibly be reduced by increasing the number of neutron histories, but some of the noise might also be attributed

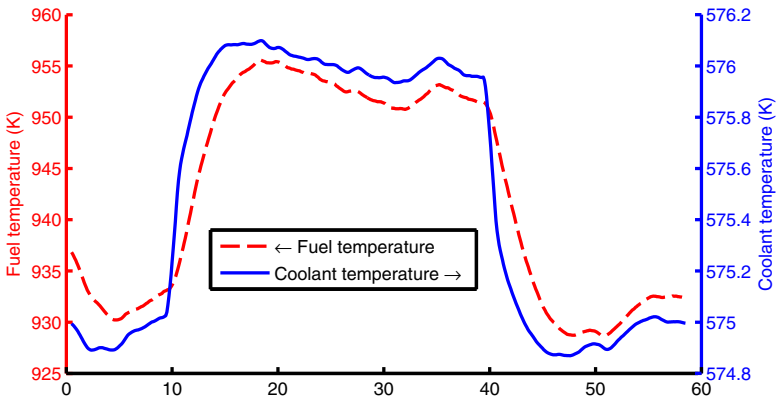

Fig. 11. The axial temperature profiles of the fuel and coolant are plotted. It can be seen that the transient is initiated by the change in coolant temperature and therefore the coolant density.

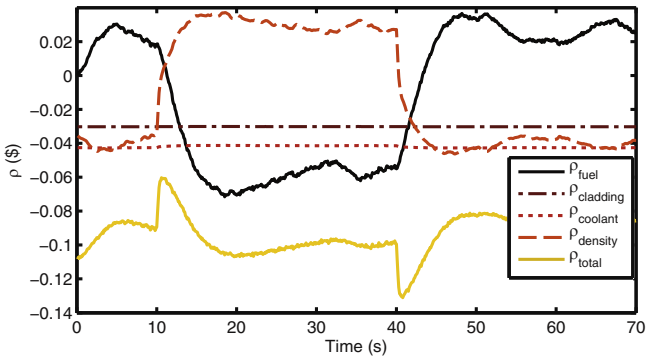

Fig. 13. The evolution of the reactivity, calculated using average temperatures and density It can be observed how the effect of the density change and the fuel temperature cancel each other.

to the step size in the coupling scheme. This can add to the uncertainty in the result. However, it is still unknown if the results are valid; to verify the new method, a comparison with other codes is needed.

3.3. NURISP benchmark

3.3.1. Problem setup

For the final test, a benchmark problem defined in report D3.1.2.2 of the European NURISP project (Kliem et al., 2011) is analysed, which consists of a steady-state calculation and a transient calculation in a mini-core. As part of the transient calculation, a second steady-state calculation is needed to determine the critical boron concentration and from this critical state an unprotected rod-ejection accident is simulated. The fact that the transient is unprotected indicates that no external measures are being taken after the control-rod ejection.

The mini-core is taken from the benchmark described by Kliem et al. (2011) and this benchmark is based upon the OECD benchmark for MOX/UO2 core transients (Kozlowski and Downar, 2003). In the system there are two types of fuel assemblies: one with MOX fuel and one with UO_2 fuel. The mini core consists of nine fuel assemblies, from which eight contain MOX and the central fuel assembly contains UO_2. The whole set up is surrounded by water reflectors, as depicted in Fig. 14. Each assembly has 17×17 rod positions, which contains different kind of rods, as depicted in Figs. 15 and 16. The dimension of a fuel assembly is 21.42 cm, the height is 366 cm and the pitch between the rods is 1.26 cm. The control rods are only present in the UO_2 fuel assembly.

The geometry of the different types of rods can be found in Fig. 17 together with Table 2 and the dimensions can be found in Table 3 and this layout is modelled in full detail. The nuclide densities in the materials can be found in Table 4 and cross section are taken from the JEFF3.1.1 evaluations (Santamarina et al., 2009). Other boundary conditions can be found in Table 1. The exact nuclide densities in the coolant will change, depending on the results of the thermal-hydraulics calculation.

To model the geometry in detail, including all separate fuel pins, cladding, burnable-poison coatings, etc., the dynamic version of Tripoli is extended to incorporate ROOT geometry. ROOT is a framework for data processing, which also has an extensive geometry package (Brun and Rademakers, 1997) and Tripoli 4.7 can handle ROOT-geometry as input, but some alterations are made, to incorporate geometry updates throughout the calculation in the dynamic version. With the ROOT geometry it is possible to create complex geometries.

First, a test calculation is performed to see if the geometry is implemented correctly. The test calculation consists of a

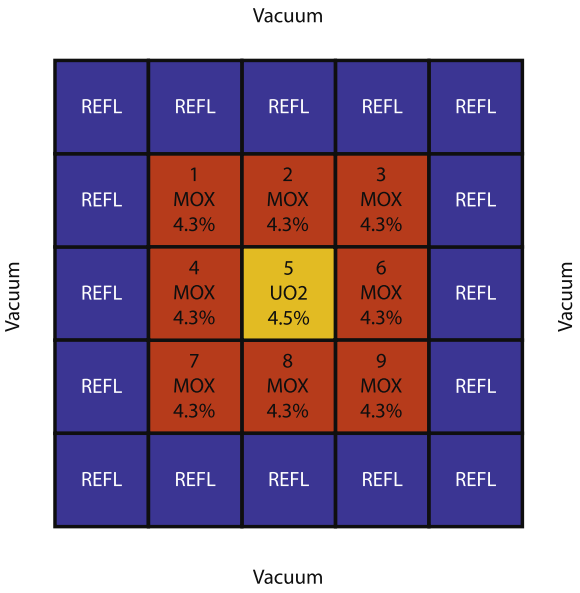

Fig. 14. The layout of the fuel assemblies in the mini core. To distinguish between the different fuel assemblies they have been assigned a number.

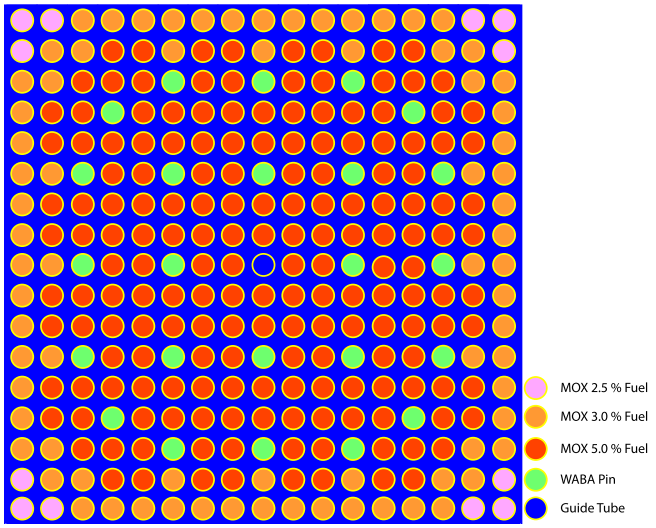

Fig. 15. The rod configuration of the MOX containing fuel assembly.

steady-state calculation at hot full power, with the control rods completely withdrawn. The results can be compared with the results calculated using DYN3D coupled with FLICA4 (Gomez-Torres et al., 2012; Jiménez et al., 2012).

3.3.2. Results

First, the hot full power calculation of the benchmark is performed with the power level fixed at 100 MW; the resulting axial power profile in the central fuel assembly is plotted in Fig. 18. It shows that the power distribution calculated with both methods agree reasonably well. In Figs. 19 and 20 the temperature and density of the coolant is plotted and also these quantities agree fairly well; similar differences can be found between coupled steady-state calculations both using Monte Carlo, but with different codes (Hoogenboom et al., 2011). The k_{eff} calculated with DYN3D-FLICA4 is 1.00828, and with Tripoli4-SubChanFlow this value is 1.01800.

The differences between the two methods might be attributed to the two different thermal-hydraulics solvers used. SubChanFlow is a quasi 3D subchannel code, solving the mass, momentum and

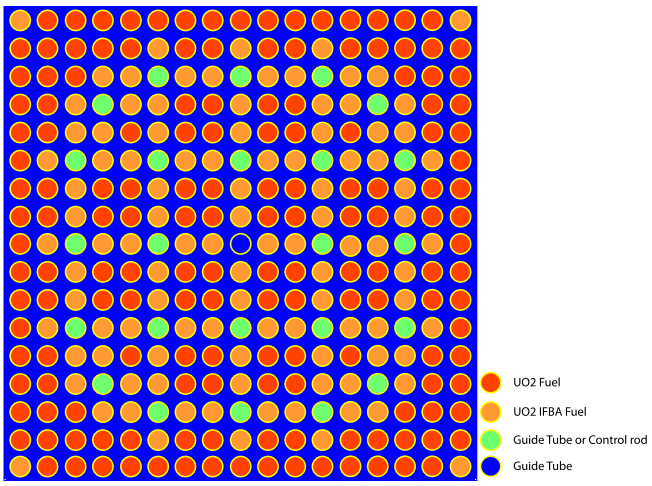

Fig. 16. The rod configuration of the UO_2 containing fuel assembly.

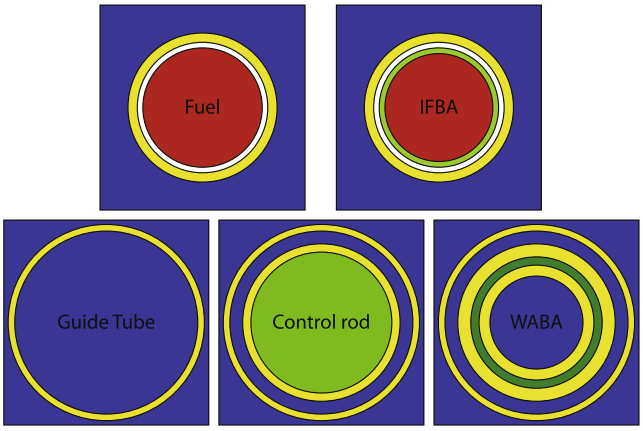

Fig. 17. The layout of the rods in the mini core.

Table 1
System properties for hot full power (HFP) and hot zero power (HZP).

Boundary conditions HFP	
Core power	100 MW
Mass flow rate (core)	739.08 kg/s
Mass flow rate (FA)	82.12 kg/s
Core Outlet pressure	15.40 Mpa
Coolant inlet temperature	560 K
Boron concentration	200 ppm (nuclide density)
Insertion depth control rods	0.0 cm
Boundary conditions HZP	
Core Power	1 W
Mass flow rate (core)	739.08 kg/s
Mass flow rate (FA)	82.12 kg/s
Core Outlet pressure	15.40 Mpa
Coolant inlet temperature	560 K
k_{eff} ($t = 0$ s)	1.0000
Insertion depth control rods	232.433 cm
Scenario	CR ejection, linear speed fully out at 0.1 s

energy equations based on the three-equation approach. On the other hand, FLICA4 is a 3D two-phase flow code (Toumi et al., 2000), where the two-phase mixture is modelled using a set of four balance equations (mass, momentum and energy of mixture and mass of vapour). It is perceivable that the two methods yield a slightly different result.

Table 2
Rod materials.

	Fuel	IFBA	GT	CR	WABA
r0-r1	Fuel	Fuel	Water	Cr	Water
r1-r2	Gap	Ifba	Clad	Clad	Clad
r2-r3	Clad	Gap		Water	Waba
r3-r4		Clad		Clad	Clad
r4-r5					Water
r5-r6					Clad

Table 3
Rod dimensions in cm.

	Fuel	IFBA	GT	CR	WABA
r1	0.3951	0.3951	0.5624	0.4331	0.2858
r2	0.4010	0.3991	0.6032	0.4839	0.3531
r3	0.4583	0.4010		0.5624	0.4039
r4		0.4583		0.6032	0.4839
r5					0.5624
r6					0.6032

After verifying the coupled-code system with the steady-state calculation, the transient analysis can be performed. The first step of a transient calculation is the determination of the initial conditions. This is achieved by calculating the critical boron concentration using iterative steady-state calculation at a power of 1 W, as explained in Section 2.2. Due to the low power, the thermal-hydraulic calculations are straight forward, so once the critical boron concentration is found the actual transient can be started.

At the start of the transient calculation, the control rods are at a partially inserted position in the central fuel assembly. Then the control rods are ejected during the first 0.1 s of the calculation, creating a large reactivity insertion. The power production in the mini core is simulated for 0.2 s and the resulting transient can be found in Fig. 21.

It can be seen that the total power level increases more than 10 decades and the highest power level is reached before the control rods are fully ejected. It can also be seen that during the power increase the two calculations have very similar results. It is only when the thermal-hydraulic effects become dominant that the two different methods start to deviate. The deviation may have the same origin as in the steady-state calculation, but the effects of the applied time grid can also influence the width of the peak (Zerkak et al., 2011). Two other calculations have been plotted in this graph, to demonstrate the variation in the results of the deterministic methods. When either the thermal-hydraulic part is replaced by a different code, or the neutronic part is replaced, the results demonstrate a variation with the same magnitude as the difference between the Monte Carlo solution and the deterministic solutions.

In Fig. 22 the evolution of the power profile in the central fuel assembly can be seen. The location where the maximum power is produced, starts at the bottom, due to the control rods which are inserted from the top. Then, as the control rods are withdrawn, the maximum starts to move upwards. A 3D-visualisation of the power profile per fuel assembly at the start of the transient is depicted in Fig. 23, which demonstrates that the power peak is located in the central fuel assembly, even with the presence of the control rods in this assembly.

In Figs. 24 and 25 the fuel temperature and moderator density evolutions can be seen, respectively. It demonstrates that the fuel temperature responds more direct to the transient power than the coolant density. Also, the response per fuel assembly is plotted, showing the impact of the control-rod movement in the central fuel assembly on the outer fuel assemblies.

Table 4
Materials used in the mini core in mol/ cm^3.

UO_2		MOX 2.5 %		MOX 3.0 %		MOX 5.0 %	
^{235}U	1.73×10^{-3}	^{234}U	7.65×10^{-7}	^{234}U	7.61×10^{-7}	^{234}U	7.45×10^{-7}
^{238}U	3.62×10^{-2}	^{235}U	7.61×10^{-5}	^{235}U	7.57×10^{-5}	^{235}U	7.42×10^{-5}
^{16}O	7.59×10^{-2}	^{236}U	3.79×10^{-7}	^{236}U	3.77×10^{-7}	^{236}U	3.69×10^{-7}
		^{238}U	3.75×10^{-2}	^{238}U	3.73×10^{-2}	^{238}U	3.65×10^{-2}
		^{239}Pu	8.98×10^{-4}	^{239}Pu	1.08×10^{-3}	^{239}Pu	1.80×10^{-3}
		^{240}Pu	5.64×10^{-5}	^{240}Pu	6.77×10^{-5}	^{240}Pu	1.13×10^{-4}
		^{241}Pu	3.81×10^{-6}	^{241}Pu	4.57×10^{-6}	^{241}Pu	7.61×10^{-6}
		^{242}Pu	9.48×10^{-7}	^{242}Pu	1.14×10^{-6}	^{242}Pu	1.90×10^{-6}
		^{16}O	7.71×10^{-2}	^{16}O	7.71×10^{-2}	^{16}O	7.71×10^{-2}

WABA		Control rod		IFBA	
C	6.46×10^{-3}	C	3.34×10^{-2}	^{90}Zr	7.71×10^{-3}
^{10}B	5.54×10^{-3}	^{10}B	2.86×10^{-2}	^{91}Zr	1.68×10^{-3}
^{11}B	2.03×10^{-2}	^{11}B	1.05×10^{-1}	^{92}Zr	2.57×10^{-3}
^{27}Al	6.29×10^{-2}			^{94}Zr	2.60×10^{-3}
^{16}O	9.44×10^{-2}			^{96}Zr	4.19×10^{-4}
				^{10}B	6.43×10^{-3}
				^{11}B	2.35×10^{-2}

Gap		Cladding				Coolant (560 K, 200 ppm boron)	
^{16}O	6.25×10^{-5}	^{90}Zr	3.60×10^{-2}	^{54}Fe	8.17×10^{-6}	^{1}H in H_2O	8.35×10^{-2}
		^{91}Zr	7.86×10^{-3}	^{56}Fe	1.28×10^{-4}	^{16}O	4.16×10^{-2}
		^{92}Zr	1.20×10^{-2}	^{57}Fe	2.96×10^{-6}	^{10}B	5.38×10^{-6}
		^{94}Zr	1.22×10^{-2}	^{58}Fe	3.94×10^{-7}	^{11}B	1.97×10^{-5}
		^{96}Zr	1.96×10^{-3}	^{50}Cr	5.44×10^{-6}		
		^{112}Sn	7.97×10^{-6}	^{52}Cr	1.05×10^{-4}		
		^{114}Sn	5.42×10^{-6}	^{53}Cr	1.19×10^{-5}		
		^{115}Sn	2.79×10^{-6}	^{54}Cr	2.96×10^{-6}		
		^{116}Sn	1.19×10^{-4}	^{14}N	2.31×10^{-4}		
		^{117}Sn	6.31×10^{-5}	^{15}N	8.54×10^{-7}		
		^{118}Sn	1.99×10^{-4}	^{122}Sn	3.81×10^{-5}		
		^{119}Sn	7.06×10^{-5}	^{124}Sn	4.76×10^{-5}		
		^{120}Sn	2.68×10^{-4}				

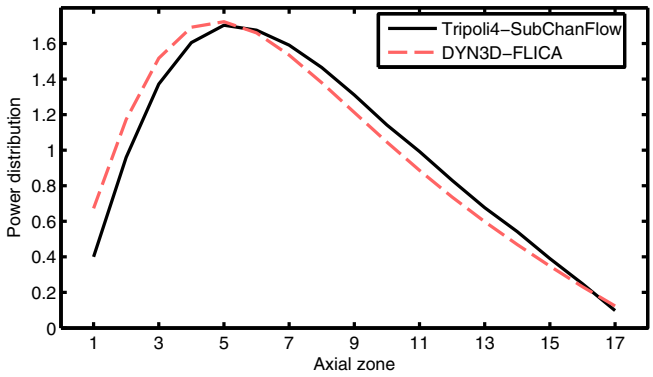

Fig. 18. The power profile in the central fuel assembly at hot full power. A small discrepancy can be seen between the two different code systems.

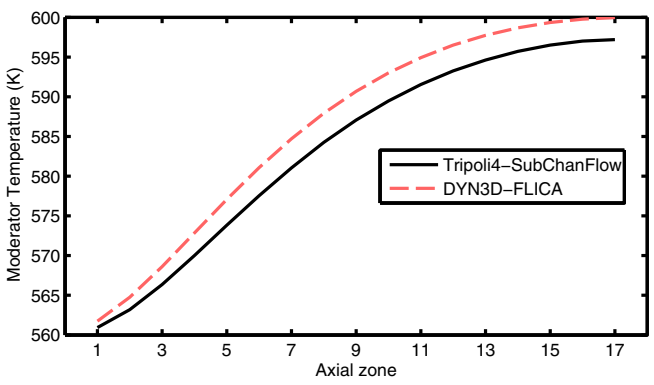

Fig. 19. The temperature profile of the moderator in the central fuel assembly at hot full power. A small discrepancy (less than 5 K) can be seen between the two different code systems.

4. Conclusions and further work

The method presented in this work is a new method, which makes it possible to calculate a transient problem with the exact and detailed modelling of the geometry and with continuous energy. This accuracy makes the method very suitable as a validation tool for other computational methods.

The calculations performed so far, all agree nicely with existing deterministic methods, which might imply that the Monte Carlo method is a more expensive way to calculate problems that can already be solved. However, these problems have been selected to be solvable by deterministic methods, creating a convincing example of the validity of the new Monte Carlo code.

Another major advantage of the Monte Carlo method is that no system-specific approximations are used and therefore it is generally applicable. It can solve not only these transient problems, but also transient problems in new reactor types, such as the

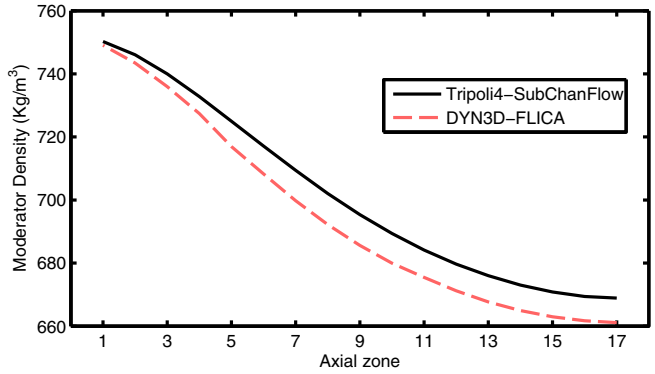

Fig. 20. The density profile of the moderator in the central fuel assembly at hot full power. A small discrepancy (less than 10 K) can be seen between the two different code systems.

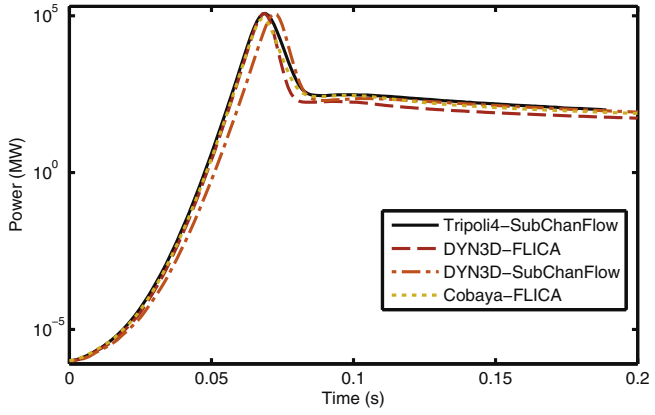

Fig. 21. The total power during the transient reaches a peak before the control rods are fully ejected. The feedback mechanisms then have a larger reactivity effect than the further withdrawal of the control rods. Although the deterministic techniques do not fully agree, it can be seen that the Monte Carlo results agree within the uncertainty of these deterministic results.

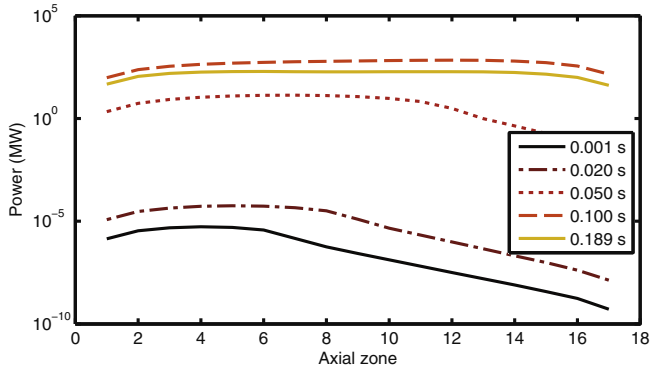

Fig. 22. The power profile evolution in the central fuel assembly. It can be noted that the power peak moves upwards in the core.

Accelorator Driven System MYRRHA, which is being designed at SCK•CEN (Aït Abderrahim et al., 2001). Due to the spallation neutrons with a very high energy this is difficult to model with the standard deterministic tools. Also unique research reactors can be complicated for deterministic tools. An example is the Fors-

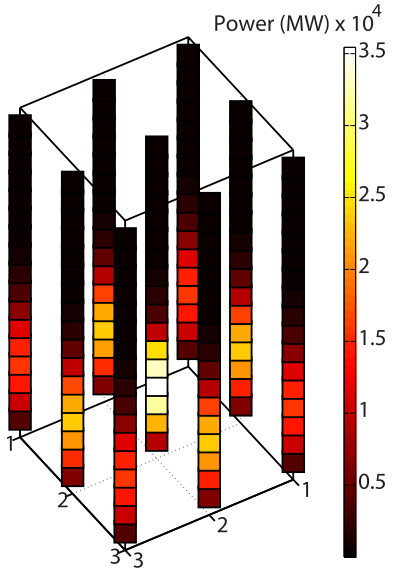

Fig. 23. The normalised power profile after 0.001 s. Each bar depicts a fuel assembly and the 3D power profile can be seen. In the beginning of the transient the power peak is located near the bottom due to the control rods. It can also be seen that most of the power is produced in the central fuel assembly.

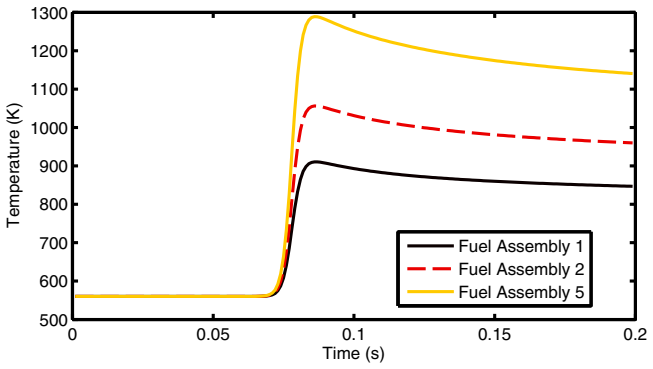

Fig. 24. The time evolution of the average temperature in the fuel pins. It can be noted that the pins heat up quickly, but the cooling is more gradual. The central fuel assembly (5) reaches the highest temperature and the fuel assemblies at the corners (1) remain the coolest. The assembly numbers can be found in Fig. 14.

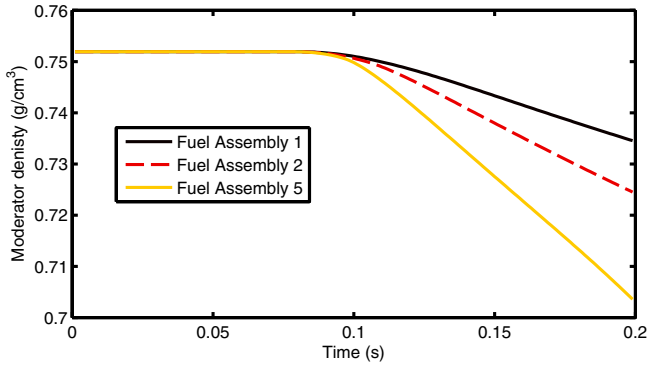

Fig. 25. The time evolution of the average moderator density. When comparing this with Fig. 24, it can be noted that the change in moderator density is much slower than the heating of the fuel pins. The assembly numbers can be found in Fig. 14.

chungs-Neutronenquelle Heinz Maier-Leibnitz at TUM (Breitkreutz, 2010; Däubler, 2012). Here the problem lies in the large distribution of neutron lifetimes due to the large heavy water reflectors.

Due to the high computational cost, its main application will be to act as a validation tool for the computationally less expensive deterministic methods. For example, the calculation of the transient in the mini core has taken one week on 28 cores on a small computer cluster.

4.1. Future work

4.1.1. Validation

The calculations shown in this paper demonstrate the feasibility of performing a coupled Monte Carlo neutronics/thermal-hydraulics calculation, even in a realistic geometry. However, it has not been possible yet to validate these calculations completely, even though the results compare well with the DYN3D-FLICA4 results. A future challenge lies in the validation of the dynamic Monte Carlo method and its implementation in the Tripoli code. The method should be benchmarked against real-life, well-documented experiments.

Furthermore, it is necessary to further investigate the effects of the variance on the coupling mechanism. It would be ideal if a theoretical description can be found to determine the validity of the estimation of the mean and the variance.

Also, the method of tallying the produced power must be further investigated. In this paper the variance is calculated between batches of neutrons and the thermal-hydraulic conditions are calculated per batch. To validate the results, it is advised to investigate the results of a tally, which should have a normal distribution. If this is not the case, the central limit theorem is not valid.

If the results do not have a normal distribution, which could be the case for a reactor with flashing channels, it might prove meaningful to tally also a different quantity in addition to the power profile. For example, the maximum power peak reached during the transient disregarding the exact location of the peak could be tracked or the time it takes to reach a power peak. The regular power tally is of course still needed for the coupling with the thermal-hydraulics code.

4.1.2. Further development

Some parts of the method can be improved. Since this work is the first attempt to couple a stochastic neutronics code for transient analysis to a thermal-hydraulics code, simple schemes and techniques have been used for the coupling. After this demonstration, the next step is to further improve the simulation scheme and Monte Carlo techniques.

The Monte Carlo part of the calculation can be improved with better use of weight windows. In this work the weight windows have only been adjusted per time interval. The efficiency of the calculation can be improved when proper weight windows are applied, preferably in an automated fashion. This way the weight windows can be optimised not only in the temporal variation, but also in the other dimensions of phase space.

Another neutronics improvement can be found in the generation of temp-erature-dependent cross sections. Multiple new techniques are already successfully applied for accurate temperature modelling in steady-state Monte Carlo thermal-hydraulics coupling and one of these new ways can also make the dynamic simulation more accurate.

The geometry, temperatures and densities can be made time dependent to further improve the coupling. In the current implementation the system properties are piecewise constant, with a step at the time boundaries, but this is not compulsory for the method. The time dependence during a time interval can be implemented for externally induced changes to the system, such as the movement of a control rod, but also for results coming from the coupling, such as the temperature profile. This last feature is especially useful when using a (semi-) implicit coupling scheme.

Furthermore, the thermal-hydraulics part of the calculation can be improved. In this work a sub-channel code has been used for the thermal-hydraulics, but there are higher-fidelity computational-fluid-dynamics codes available. During the development of the coupling scheme, the efficiency of the sub-channel code is useful, but it is more logical to couple a high-fidelity neutronics method like Monte Carlo, with a high-fidelity thermal-hydraulics code.

Finally, the coupling scheme can be further improved. For example, an implicit scheme can be used for the coupling. This can be achieved by storing a copy of the particles at the start of a time interval and use these copies to start iterating per time interval. Also the data transfer becomes large when extending the method to full core calculations, with separate temperatures for all axial and radial zones of the fuel pins. Therefore integrating neutronics and thermal-hydraulics further can be an interesting option, enabling internal coupling and automated geometry mapping between the two codes.

4.1.3. Application of dynamic Monte Carlo

All in all, it has been shown that it is feasible to perform dynamic Monte Carlo analyses on nuclear systems. The main task is now to make this method generally available, so it can be tested on many different applications for further refinement.

Acknowledgements

This work is partially funded by the Integrated Project NURISP (contract n° 232124) in the 7th Euratom Framework Programme of the European Union.

References

Aït Abderrahim, H., Kupschus, P., Malambu, E., Benoit, P., Van Tichelen, K., Arien, B., Vermeersch, F., Dhondt, P., Jongen, Y., Ternier, S., et al., 2001. Myrrha: A multipurpose accelerator driven system for research & development. Nucl. Instrum. Meth. Phys. Res. Sect. A 463, 487–494.

Armishaw, M.J., Davies, N., Bird, A.J., Cooper, A.J., 2011. The ANSWERS code MONK-a new approach to scoring, tracking, modelling and visualisation. In: Proceedings of 9th International Conference on Nuclear Criticality Safety (ICNC 2011), Edinburgh, UK.

Bakanov, V.V., Zhitnik, A.K., Motlokhov, V.N., Ognev, S.P., Romanov, V.I., Ryabov, A.A., Tarasov, V.A., Tareev, S.A., Fomin, V.P., Weber, D.P., Taiwo, T.A., Yang, W.S., 2004. TDMCC Monte-Carlo package coupled with STAR-CD thermal-hydraulics code. In: Transactions of the American Nuclear Society, pp. 250–251.

Boer, B., Lathouwers, D., Kloosterman, J.L., van der Hagen, T.H.J.J., Strydom, G., 2010. Validation of the DALTON-THERMIX code system with transient analyses of the HTR-10 and application to the PBMR. Nuclear Technol. 170, 306–321.

Breitkreutz, H., 2010. Coupled Neutronics and Thermal Hydraulics of High Density Cores at FRM II. Ph.D. thesis. Technische Univeristät München.

Broeders, C.H.M., Sanchez, V., Stein, E., Travleev, A., 2003. Validation of coupled neutron physics and thermal-hydraulics analysis for HPLWR. In: Proceedings of ICAPP03, Cordoba, Spain.

Brown, F.B., Kiedrowski, B.C., Brown, D., Martin, W.R., Griesheimer, D., 2008. Advanced Monte Carlo for reactor physics core analysis. In: Workshop at PHYSOR-2008, Interlaken, Switzerland, pp. 14–19.

Brun, R., Rademakers, F., 1997. ROOT – an object oriented data analysis framework. Nucl. Instrum. Meth. Phys. Res., Sect. A 389, 81–86.

Däubler, M., 2012. New Approach to Safety Analysis of FRM II. Master's thesis. Technische Univeristät München.

D'Auria et al., F., 2004. Neutronics/Thermal-Hydraulics Coupling in LWR Technology, vol. 1. Technical Report. OECD/NEA.

Donnelly, J.V., 2011. Interpolation of temperature-dependent nuclide data in MCNP. Nucl. Sci. Eng. 168, 180–184.

Dufek, J., Gudowski, W., 2006. Stochastic approximation for Monte Carlo calculation of steady-state conditions in thermal reactors. Nucl. Sci. Eng. 152, 274–283.

Dumonteil, E., Diop, C.M., 2011. Biases and statistical errors in Monte Carlo burnup calculations: An unbiased stochastic scheme to solve Boltzmann/Bateman coupled equations. Nucl. Sci. Eng. 167, 165–170.

Espel, F.P., Avramova, M.N., Ivanov, K.N., Misu, S., 2013. New developments of the MCNP/CTF/NEM/NJOY code system – Monte Carlo based coupled code for high accuracy modeling. Ann. Nucl. Energy 51, 18–26.

Gomez-Torres, A.M., Sanchez-Espinoza, V.H., Ivanov, K., MacIan-Juan, R., 2012. DYNSUB: A high fidelity coupled code system for the evaluation of local safety parameters – part I: development, implementation and verification. Ann. Nucl. Energy 48, 123–129.

Griesheimer, D.P., Gill, D.F., Lane, J.W., Aumiller, D.L., 2008. An integrated thermal hydraulic feedback method for Monte Carlo reactor calculations. In: Proceedings of PHYSOR-2008 – American Nuclear Society Topical Meeting on Reactor Physics.

Hoogenboom, J.E., Ivanov, A., Sanchez, V., Diop, C., 2011. A flexible coupling scheme for Monte Carlo and thermal-hydraulics codes. In: Proceedings of M&C 2011 conference, Rio de Janeiro.

Hursin, M., Downar, T.J., Kochunas, B., 2011. Analysis of the core power response during a PWR rod ejection transient using the PARCS nodal code and the DeCART MOC code. Nucl. Sci. Eng. 170, 151–167.

Imke, U., Sanchez, V.H., 2012. Validation of the subchannel code SUBCHANFLOW using the NUPEC PWR tests (PSBT). Science and Technology of Nuclear Installations 2012. Article ID 465059.

Ivanov, A., Sanchez, V., Imke, U., 2011. Development of a coupling scheme between MCNP5 and SUBCHANFLOW for the pin- and fuel assembly-wise simulation of LWR and innovative reactors. In: Proceedings of M&C 2011 Conference, Rio de Janeiro.

Ivanov, K., Avramova, M., 2007. Challenges in coupled thermal-hydraulics and neutronics simulations for LWR safety analysis. Ann. Nucl. Energy 34, 501–513.

Jiménez, J., Gomez-Torres, A., Sanchez, V.H., 2012. Solutions to exercises of Boron Dilution benchmark by DYN3D/FLICA4 coupled codes at pin level. Technical Report D3.1.2.3c. NURISP.

Joo, H.G., Cho, J.Y., Kim, K.Y., Chang, M.H., Han, B.S., Kim, C.H., 2004. Consistent comparison of Monte Carlo and whole-core transport solutions for cores with thermal feedback. In: Proceedings of the PHYSOR 2004: The Physics of Fuel Cycles and Advanced Nuclear Systems - Global Developments, pp. 35–47.

Kliem, S., Mittag, S., Gommlich, A., Apanasevich, P., 2011. Definition of a PWR boron dilution benchmark. Technical Report D3.1.2.2. NURISP.

Kópházi, J., Lathouwers, D., Kloosterman, J.L., 2009. Development of a three-dimensional time-dependent calculation scheme for molten salt reactors and validation of the measurement data of the molten salt reactor experiment. Nucl. Sci. Eng. 163, 118–131.

Kotlyar, D., Shaposhnik, Y., Fridman, E., Shwageraus, E., 2011. Coupled neutronic thermo-hydraulic analysis of full PWR core with Monte-Carlo based BGCore system. Nucl. Eng. Des. 241, 3777–3786.

Kozlowski, T., Downar, T.J., 2003. OECD/NEA and U.S. NRC PWR MOX/UO2 core transient benchmark.

Legrady, D., Hoogenboom, J.E., 2008. Scouting the feasibility of Monte Carlo reactor dynamics simulations. In: Proceedings of PHYSOR-2008 - American Nuclear Society Topical Meeting on Reactor Physics, Interlaken.

Leppänen, J., Viitanen, T., Valtavirta, V., 2012. Multi-physics coupling scheme in the Serpent 2 Monte Carlo code. Trans. Am. Nucl. Soc. 107, 1165.

Mahadevan, V.S., Ragusa, J.C., Mousseau, V.A., 2011. A verification exercise in multiphysics simulations for coupled reactor physics calculations. Prog. Nucl. Energy.

Mori, M., Maschek, W., Laurien, E., Morita, K., 2003. Monte-Carlo/Simmer-III reactivity coefficients calculations for the supercritical water fast reactor. In: Proceedings of Global 2003: Atoms for Prosperity: Updating Eisenhowers Global Vision for Nuclear Energy, pp. 1754–1762.

Peltonen, J., Kozlowski, T., 2011. Development of effective algorithm for coupled thermal-hydraulic-neutron-kinetics analysis of reactivity transient. Nucl. Technol. 176, 195–210.

Ragusa, J.C., Mahadevan, V.S., 2009. Consistent and accurate schemes for coupled neutronics thermal-hydraulics reactor analysis. Nucl. Eng. Des. 239, 566–579.

Rowlands, G., 1962. Resonance absorption and non-uniform temperature distributions. J. Nucl. Energy, Parts A & B. Reactor Sci. Technol., 16.

Sanchez, V., Al-Hamry, A., 2009. Development of a coupling scheme between MCNP and COBRA-TF for the prediction of the pin power of a PWR fuel assembly. In: Proceedings of American Nuclear Society – International Conference on Mathematics, Computational Methods and Reactor Physics 2009, M & C 2009.

Santamarina, A., Bernard, D., Blaise, P., *et al.*, 2009. The JEFF-3.1.1 nuclear data library. JEFF Report 22.

Seker, V., Thomas, J.W., Downar, T.J., 2007a. Reactor physics simulations with coupled Monte Carlo calculation and computational fluid dynamics, in: Proceedings of 13th International Conference on Emerging Nuclear Energy Systems 2007, ICENES 2007, pp. 345–349.

Seker, V., Thomas, J.W., Downar, T.J., 2007b. Reactor simulation with coupled Monte Carlo and computational fluid dynamics. In: Proceedings of Joint International Topical Meeting on Mathematics and Computations and Supercomputing in Nuclear Applications, M & C + SNA 2007.

Sjenitzer, B.L., 2009. Temperature Dependent Monte Carlo Simulation: Thermalization. Technical Report. Delft University of Technology/ Commissariat à l'Énergie atomique.

Sjenitzer, B.L., Hoogenboom, J.E., 2013. Dynamic Monte Carlo method for nuclear reactor kinetics calculations. Nucl. Sci. Eng. 176, 94–107.

Tippayakul, C., Avramova, M., Espel, F.P., Ivanov, K., 2008. Investigations on Monte Carlo based coupled core calculations. In: Proceedings of Societe Francaise d'Energie Nucleaire - International Congress on Advances in Nuclear Power Plants - ICAPP 2007, The Nuclear Renaissance at Work, pp. 797–806.

T'Joen, C., Rohde, M., 2012. Experimental study of the coupled thermo-hydraulic-neutronic stability of a natural circulation HPLWR. Nucl. Eng. Des. 242, 221–232.

Toumi, I., Bergeron, A., Gallo, D., Royer, E., Caruge, D., 2000. FLICA-4: a three-dimensional two-phase flow computer code with advanced numerical methods for nuclear applications. Nucl. Eng. Des. 200, 139–155.

TRIPOLI-4 Project Team, 2010. TRIPOLI-4 version 7 user guide. CEA. serma/ltsd/rt/10-4941/a edition.

Van Der Marck, S., Meulekamp, R., Hogenbirk, A., 2005. New temperature interpolation in MCNP. In: Proceedings of M&C 2005 Conference, Avignon, France.

Vazquez, M., Tsige-Tamirat, H., Ammirabile, L., Martin-Fuertes, F., 2012. Coupled neutronics thermal-hydraulics analysis using Monte Carlo and sub-channel codes. Nucl. Eng. Des. 250, 403–411.

Vedovi, J., Ivanov, K., Gan, J., Downar, T.J., Staudenmier, J., 2004. Analysis of Ringhals I stability benchmark with TRACE/PARCS: steady-state initialization, invited. Trans. Am. Nucl. Soc. 90, 560–562.

Viitanen, T., Leppänen, J., 2012. Explicit treatment of thermal motion in continuous-energy Monte Carlo tracking routines. Nucl. Sci. Eng. 171, 165–173.

Waata, C., Schulenberg, T., Cheng, X., Laurien, E., 2005a. Coupling of MCNP with sub-channel code for analysis of HPLWR fuel assembly. In: Proceedings of the 11th International Topical Meeting on Nuclear Reactor Thermal-Hydraulics (NURETH-11).

Waata, C., Schulenberg, T., Cheng, X., Starflinger, J., Bernnat, W., 2005b. Results of a coupled neutronics and thermal-hydraulics analysis of a HPLWR fuel assembly. In: Proceedings of the American Nuclear Society - International Congress on Advances in Nuclear Power Plants 2005, ICAPP'05, pp. 300–306.

Watson, J.K., Ivanov, K.N., 2012. Demonstration of implicit coupling of TRACE/PARCS using simplified one-dimensional problems. Nucl. Technol. 180, 174–190.

Yesilyurt, G., Martin, W.R., Brown, F.B., 2012. On-the-fly doppler broadening for Monte Carlo codes. Nucl. Sci. Eng. 171, 239–257.

Zerkak, O., Gajev, I., Manera, A., Kozlowski, T., Gommlich, A., Zimmer, S., Kliem, S., Crouzet, N., Zimmermann, M.A., 2011. Revisiting temporal accuracy in Neutronics/TH code coupling using the NURESIM LWR simulation platform. In: The 14th International Topical Meeting on Nuclear Reactor Thermalhydraulics (NURETH-14).

Zoia, A., Brun, E., Jouanne, C., Malvagi, F., 2013. Doppler broadening of neutron elastic scattering kernel in tripoli-4®. Ann. Nucl. Energy 54, 218–226.